IOPscience iopscience.iop.org

Home Search Collections Journals About Contact us My IOPscience

Effect of annealing on optical properties and band alignments of ZrO_2/Si(1 0 0) by nitrogen-assisted reactive sputtering

This article has been downloaded from IOPscience. Please scroll down to see the full text article.

2006 J. Phys. D: Appl. Phys. 39 5285

(http://iopscience.iop.org/0022-3727/39/24/027)

View the table of contents for this issue, or go to the journal homepage for more

Download details:
IP Address: 202.127.206.107
The article was downloaded on 29/06/2010 at 09:05

Please note that terms and conditions apply.

Institute of Physics Publishing — Journal of Physics D: Applied Physics
J. Phys. D: Appl. Phys. **39** (2006) 5285–5289 doi:10.1088/0022-3727/39/24/027

Effect of annealing on optical properties and band alignments of ZrO_2/Si(1 0 0) by nitrogen-assisted reactive sputtering

L Q Zhu[1,3], Q Fang[2], G He[1], M Liu[1] and L D Zhang[1]

[1] Key Laboratory of Materials Physics, Anhui Key Laboratory of Nanomaterials and Nanostructure, Institute of Solid State Physics, Chinese Academy of Science, PO Box 1129, Hefei 230031, People's Republic of China
[2] Electronic and Electrical Engineering and London Centre for Nanotechnology, University College London, Torrington Place, London WCIE 7JE, UK

E-mail: qzhuli2003@yahoo.com.cn

Received 1 September 2006, in final form 21 October 2006
Published 1 December 2006
Online at stacks.iop.org/JPhysD/39/5285

Abstract
ZrO_2 films were prepared by nitrogen-assisted radio frequency (RF) reactive sputtering on n-type silicon (100). Optical properties and band alignments of ZrO_2 films on Si have been investigated by using x-ray photoelectron spectroscopy (XPS) and spectroscopy ellipsometry (SE). The improved film quality was obtained after annealing in N_2/O_2 ambient with stable interfacial properties. Optical properties were analysed based on the SE fitting results. According to the valence-band spectrum results, the zero-field energy-band alignments for ZrO_2/SiO_2/Si stacks were also extracted. Our results indicate that the nitrogen-assisted process shows its outstanding ability in the control of interfaces and has potential application in microelectronics.

1. Introduction

Silicon dioxides have been used successfully in gate dielectrics application for decades. However, for 80 nm technology, the equivalent oxide thickness (EOT) of 1.2 nm for high-performance logic technology and 1.4 nm for low operating power (LOP) technology is needed. It will further drop to 0.7 nm and 0.9 nm in 2010, respectively [1]. This causes reduced dielectric reliability and significant gate leakage current [2]. As a result, research has focused recently on investigating potential alternative dielectrics with higher dielectric constant (k) than that of SiO_2 ($k = 3.9$), such as zirconium and hafnium oxides [3–6]. Unfortunately, both of them crystallize at relatively low temperatures, and there is an interfacial layer growth between high-k oxides and Si substrate at high temperature as well, which poses a serious concern to EOT scalability [7–9]. As an effective method, the nitration process impedes the crystallization of high-k oxides at high temperature [10, 11], and oxygen diffusion and boron penetration through high-k oxides have been retarded successfully [12]. Though high-k dielectrics nitrated by NH_3 are known to reduce EOT and leakage current density [10], it also causes an increase in the interface trap density and a degradation of mobility due to the hydrogen related traps (−H, −OH and N–H) [13]. Moreover, high temperature annealing always results in the outlet of nitrogen from high-k films and pileup of nitrogen in the interfacial region, which will cause potential flatband voltage shift and threshold voltage instability [14]. So it is desirable to develop an economical and safe process to prepare high-k thin films. In our early work, the nitrogen-assisted process shows its outstanding ability in the control of interfaces [15]. In an attempt to reduce the interfacial layer thickness further, ZrO_2 films were prepared on Si(100) by nitrogen-assisted radio frequency (RF) magnetron sputtering in $N_2/Ar/O_2$ ambient.

2. Experimental process

2.1. Sample preparation

Zirconia films were deposited on single-crystal Si substrates (n-type, (100) orientation, $\rho = 1$–$10\,\Omega\,$cm) by nitrogen-assisted RF magnetron sputtering from a zirconium target (99.99%) without any intentional heating. The Si

[3] Author to whom any correspondence should be addressed.

0022-3727/06/245285+05$30.00 © 2006 IOP Publishing Ltd Printed in the UK

substrates were pre-ultrasonically cleaned in a solution ($NH_3{\cdot}H_2O:H_2O_2:H_2O = 2:1:7$) for 20 min to remove organic, then rinsed in de-ionized water; after that the Si substrates were dipped in a 4%HF solution to remove the native silicon oxide on surface and form a hydrogen-terminated surface. The base pressure was about 3.6×10^{-4} Pa. The working plasma was excited by a 13.56 MHz radio frequency. During the sputtering, the distance between the substrate and target was fixed at 4.0 cm and the plasma power at $3.9\,\mathrm{W\,cm^{-2}}$. The high purity (99.999%) gas flow rate in the deposition chamber was set to 60 sccm ($N_2 = 30$ sccm; $O_2 = 10$ sccm; Ar = 20 sccm) and chamber pressure at 0.2 Pa. The zirconium metal target was pre-sputtered for 10 min in order to remove the surface contaminants on the target and stabilize the sputtering. To evaluate the oxides' response to the *ex situ* thermal annealing, the as-deposited zirconia films were subjected to post-deposition annealing at different temperatures for 5 min in high purity (99.999%) N_2/O_2 (N_2: 98 sccm, O_2: 2 sccm) by rapid thermal annealing (RTA).

2.2. Film characterization and ellipsometry procedures

The surface chemical bond states of the samples were analysed by means of x-ray photoelectron spectroscopy (XPS) using the ESCALAB MK II (VG, UK) system, equipped with an Mg K_α radiation source (1253.6 eV). The binding energies of the core levels were calibrated by setting the adventitious C1s peak at 284.6 eV in our case. The thickness and optical properties of the films were deduced by using an *ex situ* spectroscopic phase-modulated ellipsometry (Model UVISE JOBIN-YVON).

Spectroscopic ellipsometry (SE) is a nondestructive and powerful technique to investigate the optical response of materials and, in particular, to measure simultaneously the thickness and the optical constants of a multi-layer system when appropriate modelling approaches have been developed. Ellipsometric data (IS/IC) were obtained at an incidence angle of 70° across the spectral range 0.75–6.5 eV. IS and IC are related to the ellipsometric angles ψ and Δ defined in the fundamental equation of ellipsometry as follows [16]:

$$\rho = r_P/r_s = \tan\,\psi \cdot \exp(\mathrm{i}\Delta), \quad (1)$$

$$\mathrm{IS} = \sin(2\psi)\sin(\Delta), \quad (2)$$

$$\mathrm{IC} = \sin(2\psi)\cos(\Delta), \quad (3)$$

where the s-component is oscillating perpendicular to the plane of incidence and the p-component is oscillating parallel to the plane of incidence. r_p and r_s are the complex Fresnel reflection coefficients, parallel and perpendicular to the plane of incidence, respectively. The spectroscopic measurements exhibit two different processes. In the data collection process, the experimental SE data (IS/IC) are obtained, while the fitting process is used to adjust the theoretical fitting coefficients to the experimental data until the best fit is obtained through χ^2 (goodness of fit) minimization process. Both the film optical constant and thickness were extracted from the SE data analysis simultaneously. The optical constants of zirconia films were determined using the new-amorphous dispersion formula [17]. A classical dispersion model relation was used to describe the unknown optical constant of interfacial layer. Based on the SE optical band-gap energy (E_g) and XPS valence-band spectrum results, energy-band alignments were analysed.

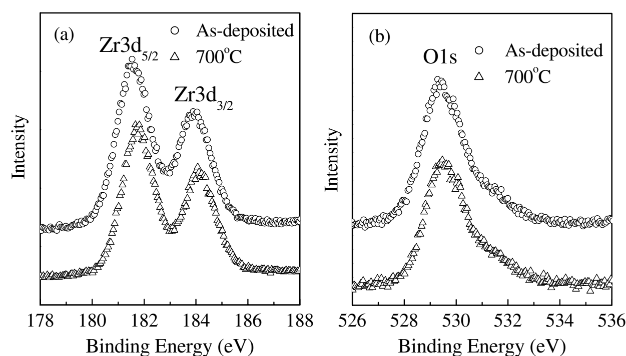

Figure 1. XPS core level spectra of Zr_{3d} and O_{1s} for ZrO_{2-x} films: (*a*) core level spectra of Zr_{3d} and (*b*) core level spectra of O_{1s}.

3. Results and discussion

3.1. Film composition

Figure 1 shows the Zr_{3d} portion and O_{1s} portion of the XPS signal. The binding energy of the $Zr3d_{5/2}$ feature in as-deposited ZrO_{2-x} is 181.5 eV, lower than that of the fully oxidized Zr in its Zr^{4+} state at 182.4 eV [18]. The lower $Zr3d_{5/2}$ binding energy may be due to the sub-oxidization in Zr states. After annealing at 700 °C, the $Zr3d_{5/2}$ peak shows a slight blue shift to 181.8 eV. The increase in $Zr3d_{5/2}$ binding energy is associated with the increased oxidization in Zr states after the additional high temperature annealing. The O_{1s} peak at around 529.6 eV is associated with the Zr–O bond. While the weak shoulder at higher binding energy is associated with adsorbed oxygen in the film or at the film surface. It is clearly seen that the O_{1s} peaks have no significant change, indicating the stable O_{1s} state. The slightly lower O_{1s} binding energy is attributed to the different atomic configuration compared with that of the stoichiometric ZrO_2. Additionally, there is no N_{1s} peak at the energy range from 392 to 408 eV for the studied samples (not shown), indicating that no nitrogen states have been incorporated into the ZrO_{2-x} matrix or that the nitrogen content in the films is below the XPS measurement accuracy.

3.2. Optical properties by spectroscopic ellipsometry

For ultra-thin layers, the accurate determination of each fitting parameter is a difficult matter because of the correlation among them. At the same time, ellipsometric characterization requires an appropriate model for stacking structure. Since an interfacial layer is always observed for ZrO_2/Si stacks [8, 9, 15] and our Fourier transform infrared spectroscopy analysis has also indicated the existence of an SiO_2 interfacial layer between ZrO_2 and Si substrates (not shown here), a four-layer model is used to extract the optical constants of the thin films: Si(100) substrates, SiO_2 interfacial layer, homogeneous ZrO_2 films and surface rough layer which was assumed to consist of 50% ZrO_2 and 50% voids based on the Bruggeman effective medium approximation (BEMA) [19]. The schematic structure of the four-layer model is shown in the inset of figure 2. In order to get a high accuracy, the thickness of the surface rough layer is set at the value ascertained from atomic force microscopy (AFM) analysis. The surface rough layer thickness is listed in table 1, which is double the AFM root-mean-square (rms) values based on Song's reports [19].

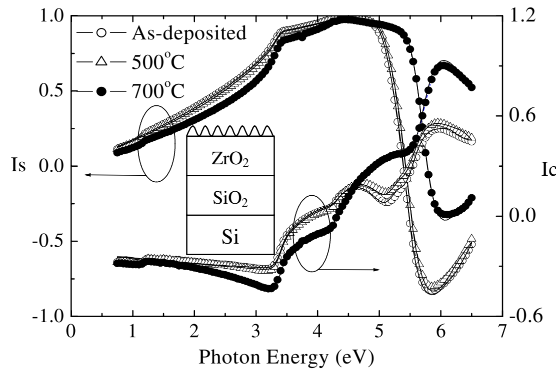

Figure 2. Experimental (dots) and fitted (solid lines) spectroscopic ellipsometry data, IS and IC. Inset shows the schematic structure of the four-layer SE model.

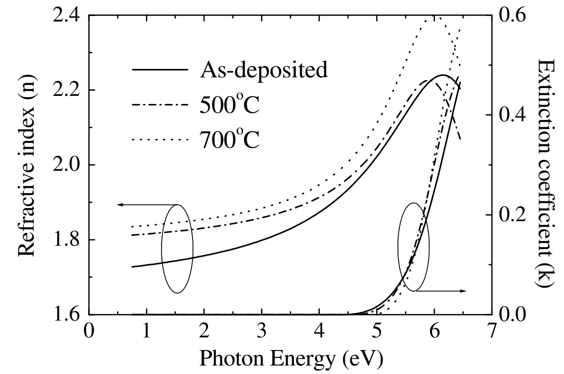

Figure 3. Extracted refractive index (n) and extinction coefficients (k) for zirconia.

Table 1. ZrO_2 spectroscopic ellipsometric fitting results. Sr represents the SE surface roughness of the ZrO_2 films. rms represents the AFM root-mean-square. χ^2 represents the goodness of fit. E_g represent the extracted optical band-gap.

Temperature (°C)	As-deposited	500 °C	700 °C
AFM rms (nm)	0.5	0.5	0.4
SE sr(nm)	1.0	1.0	0.8
Interfacial layer (nm)	1.3	1.3	1.6
ZrO_2 thickness (nm)	20.5	19.7	18.4
χ^2	1.67	1.45	1.43
E_g (eV)	5.06	5.07	5.18

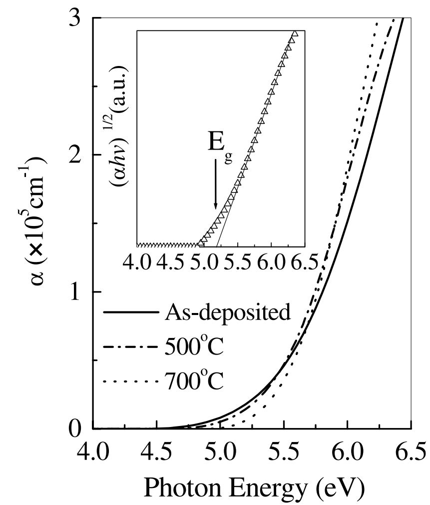

Figure 4. α versus $h\nu$ plot of as-deposited ZrO_2 films and those following annealing at high temperature. The inset figure shows the $(\alpha h\nu)^{1/2}$ versus $h\nu$ plot of 700 °C annealed ZrO_2 films. The intersection indicates the E_g value as indicated by the arrow.

Figure 2 shows the experimental (dot curves) and fitted (solid lines) data of IS and IC as a function of photon energy. Although the lowest χ^2 values are always larger than 1 (table 1), this figure confirms that the fitted curves approach the experimental data very well indicating that the physical and optical properties of the thin films are described with high precision. Additionally, the figure shows that there is a gradual change in IS and IC for ZrO_2 films after *ex situ* high temperature annealing, indicating that the optical properties are modulated by the additional annealing. Table 1 summarizes the SE fitting results. The ZrO_2 thickness shows a slight shrinking after the additional annealing, indicating the increased packing density. In our early work, there is a significant interfacial layer grown after the additional annealing for reactive sputtered ZrO_2 on Si in Ar/O_2 ambient [9]. However, the interfacial growth has been successfully retarded for nitrogen-assisted direct current reactive sputtered ZrO_2 on Si after *ex situ* high temperature annealing [15]. In this work, it is clearly seen that the interfacial thickness with a much smaller value (1.3 versus 3.0 nm in [15]) has just a slight change after the additional annealing, indicating the stable interfacial properties. Our SE results indicate that nitrogen-assisted RF reactive sputtering shows its outstanding ability in the control of interfaces.

Optical constants are considered to be a gauge of film quality. Figure 3 shows the refractive index (n) and extinction coefficient (k) as a function of photon energy calculated from the extracted best-fit coefficients of the model for the ZrO_2 films on silicon. It can be seen that the annealing temperatures have significant effects on the optical constants. Considering the Clausius–Mosotti relationship $[(n^2 - 1)/(n^2 + 2) = (4\pi/3)\alpha_{mp}/V_m$; α_{mp}: molecular polarizability; V_m: molecular volume] [20], the higher n value following annealing at high temperature may be due to the increased polarizability and decreased molecular volume after annealing. The non-zero extinction coefficient (k) at the high photon energy is related to the band–band transitions. Since k is related to the optical absorption, its value will have some change when the band-gap energy changes. It is clearly seen in figure 3 that there is a slight blue shift in the k tail edge after the additional high temperature annealing, indicating the change in the optical absorption properties.

In order to discuss the optical properties of ZrO_2 films, we studied the relationship of optical absorption coefficient and photon energy. Figure 4 shows the absorption coefficients (α), using a relationship, $\alpha = 4\pi k/\lambda$, where λ is the wavelength of a photon and k is the corresponding extinction coefficient of zirconia. It is clearly seen that there is a constant shift in the absorption tail edge, which maybe due to the annihilation of defects in the zirconia films caused by more incorporation of oxygen. Since ZrO_2 systems have an indirect gap, the inter-band absorption can be expressed by the following equation [21]:

$$\alpha h\nu \propto (h\nu - E_g)^2, \quad (4)$$

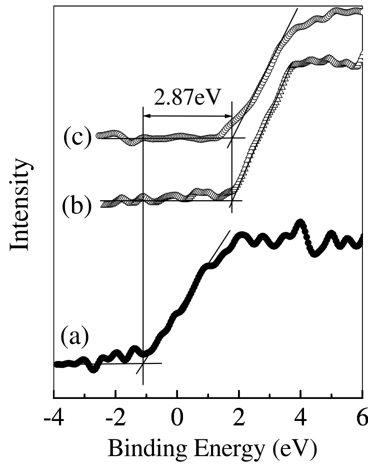

Figure 5. Valence-band spectrum for (*a*) clean Si(100) substrates, (*b*) as-deposited and (*c*) 700 °C annealed ZrO_2 films on Si.

where $h\nu$ is the incident photon energy. The $(\alpha h\nu)^{1/2}$ versus $h\nu$ curve for the annealed zirconia films is shown in the inset of figure 4. The optical band-gap energies E_g can be obtained by extrapolating the linear portion of the curves relating $(\alpha h\nu)^{1/2}$ and $h\nu$ to $(\alpha h\nu)^{1/2} = 0$. The extracted optical band-gap (E_g) shows a slight blue shift from 5.06 to 5.18 eV after the additional annealing. According to Pauling's theory [22], the increased E_g value is due to the increased stoichiometric in the ZrO_{2-x} film because of the oxidization of sub-oxidized zirconia in N_2/O_2 ambient at high temperature as has been indicated by XPS results.

3.3. Band alignments

The XPS valence-band spectrum method can be used to determine the band alignment of dielectric/semiconductor heterostructure. Figure 5 shows the XPS valence-band spectrum for as-deposited and 700 °C annealed ZrO_2 films and clean Si(100) substrates. The band edges are determined using the conventional method of linear extrapolation of the valence-band leading edge to the background intensity level. The results indicate the same valence-band offset of 2.87 eV for both samples on Si. Both x-ray absorption spectra (XAS) and local density approximation (LDA) have indicated that the top of the valence-band is derived from nonbonding π orbital of O_{2p} states and the lowest conduction bands are associated with transition metal (TM) nd states with $t_{2g}(\pi^*)$ and $e_g(\sigma^*)$ symmetries [21, 23]. Since XPS analysis indicates the same O_{1s} core level, it is reasonable for the similar valence-band leading edge of the two samples.

For $ZrO_2/SiO_2/Si$ system, the conduction-band offset can be derived:

$$\Delta E_C(ZrO_2\text{–}SiO_2) = E_g(SiO_2) - \Delta E_V(SiO_2\text{–}Si) + \Delta E_V(ZrO_2\text{–}Si) - E_g(ZrO_2), \quad (5)$$

where $\Delta E_C(ZrO_2\text{–}SiO_2)$ is the conduction-band offset of ZrO_2–SiO_2, $E_g(SiO_2)$ is the band-gap of SiO_2, $E_g(ZrO_2)$ is the band-gap of ZrO_2, $\Delta E_v(SiO_2\text{–}Si)$ is the valence-band offset of SiO_2–Si and $\Delta E_v(ZrO_2\text{–}Si)$ is the valence-band offset of ZrO_2–Si. Since there is a thin SiO_2 interfacial layer for our ZrO_2 films on Si, the energy-band alignment between SiO_2 and Si from the literature reports can be used [24]. Using valence-band spectrum results and the SE measured band-gap of ZrO_2, the zero-field conduction-band offset is determined. Figure 6 shows the zero-field energy-band alignment for as-deposited (figure 6(*a*)) and 700 °C annealed (figure 6(*b*)) $ZrO_2/SiO_2/Si$ stacks. Considering that the anti-bonding d-states of zirconium form the lowest conduction-band states in ZrO_2, the increase in Zr oxidization states results in the change in the conduction-band offset for ZrO_2–SiO_2 stacks.

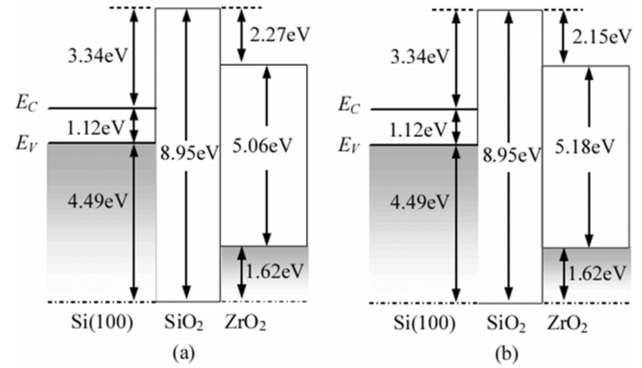

Figure 6. Zero-field energy-band alignments of $ZrO_2/SiO_2/Si$ stacks for (*a*) as-deposited and (*b*) 700 °C annealed ones, respectively. The energy-band alignment of SiO_2/Si is obtained from the results in [24].

4. Conclusions

ZrO_2 films have been prepared by nitrogen-assisted radio frequency reactive magnetron sputtering on n-type silicon (100). Film optical properties are analysed as a function of annealing temperature. The increased refractive index indicates the improved film quality after annealing. A very slight additional interfacial growth has been observed, indicating the stable interfacial properties. The slight blue shift in the extracted absorption edge indicates the increased optical band-gap. Additionally, the effects of additional annealing on the zero-field energy-band alignments for $ZrO_2/SiO_2/Si$ stacks are also extracted based on the valence-band spectrum and SE band-gap results. Our results indicate that the nitrogen-assisted process has outstanding ability in the control of interfaces and potential application in microelectronics.

Acknowledgments

This work was supported by the National Key Project of Fundamental Research for Nanomaterials and Nanostructures (Grant No 2005CB623603).

References

[1] Semiconductor Industry Association 2005 *International Technology Roadmap for Semiconductors* http://public.itrs.net

[2] Green M L, Gusev E P, Degraeve R and Garfunkel E L 2001 *J. Appl. Phys.* **90** 2057

[3] Wilk G D, Wallance R M and Anthony J M 2001 *J. Appl. Phys.* **89** 5243

[4] Wang M-T, Cheng B Y-Y and Lee J Y-M 2006 *Appl. Phys. Lett.* **88** 242905
[5] Chi D and Mclntyre P C 2004 *Appl. Phys. Lett.* **85** 4699
[6] Fang Q, Liaw I, Modreanu M, Hurley P K and Boyd I W 2005 *Microelectron. Reliab.* **45** 957
[7] He G, Fang Q, Liu M, Zhu L Q and Zhang L D 2004 *J. Cryst. Growth* **268** 155
[8] Howard J M, Craciun V, Essary C and Singh R K 2002 *Appl. Phys. Lett.* **81** 3431
[9] Zhu L Q, Fang Q, He G, M Liu and Zhang L D 2006 *Mater. Lett.* **60** 888
[10] Kim J-H, Choi K-J and Yoon S-G 2005 *Appl. Surf. Sci.* **242** 313
[11] Jeon S, Choi C-J, Seong T-Y and Hwang H 2001 *Appl. Phys. Lett.* **79** 245
[12] Choi C H, Jeon T S, Clark R and Kwong D L 2003 *IEEE Electron. Device Lett.* **24** 215
[13] Cho H J, Kang C S, Onishi K, Gopalan S, Nieh R, Choi R, Dharmarajan E and Lee J C 2001 *Int. Electron Devices Meeting (2001) Tech. Digest* p 655
[14] Kang C S, Cho H-J, Choi R, Kim Y-H, Kang C Y, Rhee S J, Choi C, Akbar M S and Lee J C 2004 *IEEE Trans. Electron. Devices* **51** 220
[15] Zhu L Q, Fang Q, He G, Liu M and Zhang L D 2005 *Nanotechnology* **16** 2865
[16] http://www.jobinyvon.com/usadivisions/TFilms/basicellip.htm
[17] Forouhi A R and Bloomer I 1986 *Phys. Rev.* B **34** 7018
[18] Guittet M J, Crocombette J P and Soyer M G 2001 *Phys. Rev.* B **63** 125117
[19] Song Z, Rogers B R and Theodore N D 2004 *J. Vac. Sci. Technol.* A **22** 711
[20] Kittel C 1986 *Introduction to Solid State Physics* (New York: Wiley)
[21] Peacock P W and Robertson J 2002 *J. Appl. Phys.* **92** 4712
[22] Pauling L 1960 *The Nature of the Chemical Bond* (Ithaca, NY: Cornell University Press)
[23] Lucovsky G, Rayner G B, Jr, Kang D, Appel G, Johnson R S, Zhang Y, Sayers D E, Ade H and Whitten J L 2001 *Appl. Phys. Lett.* **79** 1775
[24] Miyazaki S 2001 *J. Vac. Sci. Technol.* B **19** 2212